PRELIMINARY SURFACE THERMAL FLUX CALCULATIONS USING LRO DIVINER IN LUNAR PERMANENTLY SHADOWED CRATERS. C. J. Ahrens[1], N. Petro[2], M. A. Siegler[3], [1]Arkansas Center for Space and Planetary Science, Fayetteville, AR 72701 (ca006@email.uark.edu), [2]NASA Goddard Space Flight Center, Solar System Exploration Division, Greenbelt, MD, [3]Planetary Science Institute

Introduction: Volatiles are observed at several lunar polar craters, particularly the permanently shadowed regions (PSRs). Recent observations have shown certain craters appear to have asymmetries in potential ice deposits as well as variation of temperatures based on measurements from Lunar Reconnaissance Orbiter's Lunar Orbiter Laser Altimeter (LRO-LOLA), Diviner Lunar Radiometer Experiment (Diviner), and Moon Mineralogy Mapper (M^3).

Hayne et al. [1] found that many PSR's near the lunar south pole have maximum surface temperatures < 100 K, consistent with the presence of stable water ice found using LRO's Lyman Alpha Mapping Project (LAMP) [2]. Surface temperatures in these shadowed regions are largely controlled by reflected sunlight and irradiated infrared light from adjacent topography [3-6]. These areas act as cold traps, capable of accumulating water and other volatile compounds over time [7]. However, surfaces that experience temperatures > 100 K should lack surface water ice due to the temperature-dependent sublimation [8]. Relatively short time periods of higher temperatures would rapidly sublimate a surface deposit depending on its thickness [9]. Conversely, surfaces within < 100 K temperature conditions can preserve surface frost over geological time periods.

There is a current lack of understanding regarding the thermal stability and surface thermal flux of these PSRs. In this work, we measure the day and night-time bolometric temperatures from Diviner (Fig.1) over seven years (2009-2016). From these changes in day-night temperatures, we can calculate the surface thermal flux within a crater to either verify or redefine the PSR volatile ice stability. We identified four craters (two in the north pole, two in the south pole) with different extents of PSR shadow coverage for comparison.

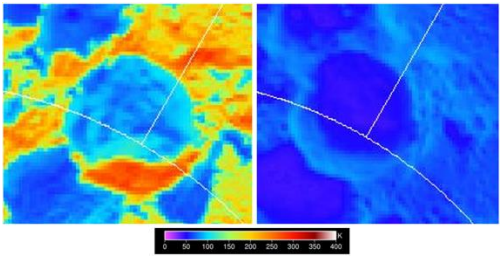

Figure 1: *Example of Diviner bolometric temperature maps for day (left) and night (right). Shown is Rozhdestvenskiy U from the study.*

Methodology: LROC Wide Angle Camera (WAC) and Diviner data were used, all publicly available on the Planetary Data System (PDS) Geosciences Node, together with the Java Mission-planning and Analysis for Remote Sensing (JMARS) software. Coincident Diviner temperature data was available at a resolution of 500 m [10]. Ten traverses were taken across each of our sample craters. The day-night bolometric temperatures were plotted from each traverse over a period of time (years 2009-2016). These temperatures were then compared to temperature-dependent water ice crystallization regimes, which are amorphous (< 140 K; though a density change within the ice matrix can occur at 77 K) and crystalline (> 140 K). These differences in crystallization (and densities) could have a profound effect in the thermal inertia and other regolith properties [11], including the stability of such volatiles over seasonal time.

Once the Diviner bolometric temperature are recorded across an impact crater, the average difference in day and night-time temperatures (ΔT) within a whole year are used to determine the heat transfer Q (in units of W):

$$Q = \frac{kA(\Delta T)}{d}$$

Where k is the thermal conductivity (used as 0.0093 ($W\ m^{-1}\ K^{-1}$) from [12], A is the area of the crater, and d is a uniform thickness (in this study, we used 0.02 m). Q is then be used to determine the surface thermal flux as:

$$Q_{IR} = \frac{Q}{A}$$

Determining the thermal surface flux of a crater provides insight into the stability of the regolith heat retention, especially for the preservation or destruction of PSR water ice and other volatiles over short timescales.

Results: *Rozhdestvenskiy U (84.8°N, 152.4°E):* After plotting the bolometric temperatures from Diviner, the PSR regions in this crater are mostly within the < 77 K region, with more stability in Traverses 6-7 (Fig. 2). After applying the bolometric day-night temperature differences (Fig. 3) to the above thermal flux equations, the lowest thermal flux values were found in Traverses 6-7 (Fig. 4), verifying the stability of the previously observed PSR locations within this crater [7].

Sylvester (82.6°N, 278.8°E): This northern crater has a comparably smaller PSR area than

Rozhdestvenskiy U. PSRs have been previously observed at Traverses 2-4 [7]. Day-night temperatures are generally 77 K, with variability up to 100 K near the crater rim. There is an observable discrepancy where Traverses 2 and 4 have the lowest thermal flux values, indicating relatively better stability than the rest of the crater. It is interesting to note that through 2009-2016 that the entirety of this crater was within the amorphous ice region, whereas Rozhdestvenskiy U is in the crystalline ice regime until the shift in amorphous ices at the PSR shadowed portion. These differences in crystallization regimes could give insight to the asymmetric morphologic properties of the craters and stability of the PSRs.

Wiechert J (85.1°S, 182.8°E): The interior of this southern crater is largely in permanent shadow, which is covered by Traverses 2-6. The majority of the day-night measured temperatures were within the higher amorphous regime < 140 K.

Amundsen (84.4°S, 86.2°E): This crater offers an interesting comparison to *Wiechert J* in that previous observations of PSRs at this crater have been made (Fig. 2) [13], but that the day-night temperature conditions are relatively more variable. However, Traverses 2-3 show a very stable ~50 K temperature region at the base of the crater wall. From the thermal flux model, this small portion of the crater may suggest a cold trap at the crater wall.

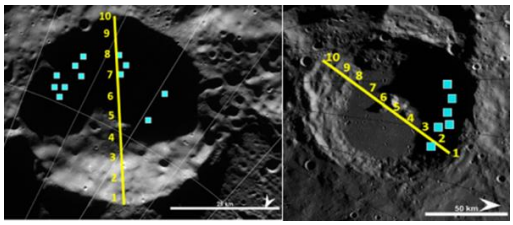

Figure 2: ***(Left)*** *LROC WAC mosaic of Rozhdestvenskiy U with traverse markers (in yellow) and PSR observations (blue squares). Scale bar at 25 km.* ***(Right)*** *Amundsen with traverse markers in yellow and previous PSR observations marked in blue. Scale bar at 50 km.*

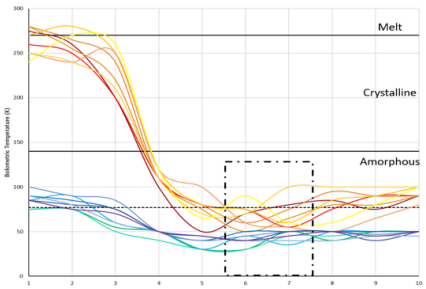

Figure 3: *Example of day and night-time bolometric temperatures from 2006-2016 of Rozhdestvenskiy U. Water ice crystallization regimes are marked. The dot-dash box indicates the most stable Traverses.*

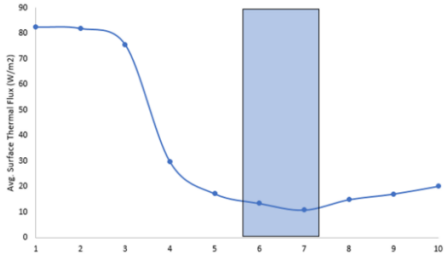

Figure 4: *Example of surface thermal flux model from Rozhdestvenskiy U Traverses. Shaded box indicates the lowest thermal flux (most stable) Traverses.*

Conclusions: We find that temperature variations associated with the accumulation of volatiles within lunar PSRs and can be verified with surface thermal flux calculations. The thermal flux measurements further our understanding of thermal stability, volatile crystallization processes, and cold trapping. Knowing the different water ice crystallization regimes gives us insight to the regolith properties and how the thermal stability of the PSRs region would influence the overall structure of the crater (i.e., morphology, ejecta volume, mass wasting, etc.). Thus, the thermal modeling used from this work could find more potential PSR regions otherwise too small (or seasonally transient) from orbiters. These PSR craters have the potential to address key lunar exploration questions, especially the perspective on volatile distribution and regolith properties outlined in the Planetary Science Decadal Survey, Visions and Voyages [14].

References: [1] Hayne, P., et al. (2015) *Icarus*, 255, 58-69. [2] Gladstone, G.R., et al. (2010) *Space Sci. Rev.*150(1-4), 161–181. [3] Watson, K., et al. (1961) *J Geophys. Res.*, 66, 3033-3045. [4] Ingersoll, A., et al. (1992) *Icarus*, 100, 40-47. [5] Salvail, J., Fanale, F., (1994) *Icarus*, 111, 441-455. [6] Vasavada, A., et al. (1999) *Icarus*, 141, 179-193. [7] Li, S., et al., (2018) *PNAS*, 115 (36), 8907-8912. [8] Andreas, E., (2007) *Icarus*, 186 (1), 24-30. [9] Paige, D., et al., (2013) *Science*, 339, 300-303. [10] Chin, G., et al. (2007) *Space Sci. Rev.*, 129 (4), 391-419. [11] Andersson, O., Inaba, A. (2005) *Phys.Chem.*, 7, 1441-1449. [12] Siegler, M., et al. (2015) *Icarus*, 255, 78-87. [13] Mazarico, E., et al. (2011) *Icarus*, 211, 1066-1081. [14] NRC (2011).